

Characterization nanosuspension formulated with *Graptophyllum pictum* (L.) Griff extract and hydroxyapatite as bone graft material: experimental laboratory study

Kavanila Bilbalqish¹
Ratri Maya Sitalaksmi²
Devi Rianti³
Khairul Anuar bin Shariff⁴

¹Master Program of Dental Health Science, Faculty of Dental Medicine, Universitas Airlangga, Indonesia

²Department of Prosthodontics, Faculty of Dental Medicine, Universitas Airlangga, Indonesia

³Department of Dental Material, Faculty of Dental Medicine, Universitas Airlangga, Indonesia

⁴School of Material and Mineral Resources Engineering, Engineering Campus, Universiti Sains Malaysia, Malaysia

*Correspondence

Email | devirianti_ss@yahoo.com

Submit | 09 April 2024

Revisi | 04 Maret 2024

Penerimaan | 20 April 2025

Publikasi Online | 30 April 2025

DOI: [10.24198/jka.v37i1.56148](https://doi.org/10.24198/jka.v37i1.56148)

p-ISSN [0854-6002](https://doi.org/10.24198/jka.v37i1.56148)

e-ISSN [2549-6514](https://doi.org/10.24198/jka.v37i1.56148)

Citation | Bilbalqish K, Sitalaksmi RM, Rianti D. Characterization nanosuspension formulated with *Graptophyllum pictum* (L.) Griff extract and hydroxyapatite as bone graft material: experimental laboratory study. *J Ked Gi Univ Padj.* 2025;37(1):1-10. DOI: [10.24198/jka.v37i1.56148](https://doi.org/10.24198/jka.v37i1.56148)



Copyright: © 2025 by authors. Submitted to *Jurnal Kedokteran Gigi Universitas Padjadjaran* for possible open access publication under the terms and conditions of the Creative Commons Attribution (CC BY) license (<https://creativecommons.org/licenses/by/4.0/>).

ABSTRACT

Introduction: Hydroxyapatite is a major component of the inorganic minerals in the hard tissues of humans and has been widely used as a biomedical ceramic material in orthopedic and dentistry applications. Adding natural ingredients such as *Graptophyllum pictum* can increase the anti-inflammatory properties due to the presence of phenolic compounds and alkaloids. The aim of this study was to determine the characterization nanosuspension formulated with *Graptophyllum pictum* (L.) Griff extract and hydroxyapatite. **Methods:** Nanosuspension were characterized using Scanning Electron Microscopy (SEM), Electron Dispersive X-ray analysis (EDX), Fourier Transform Infrared Spectroscopy (FTIR), and Liquid Chromatography Mass Spectrometry (LCMS). These evaluations were to reveal the surface morphology, elemental composition, functional groups, and identify the active metabolite of the nanosuspension. **Results:** SEM revealed the morphology agglomeration of spherical hydroxyapatite particles. The EDX analysis revealed a content of carbon, oxygen, sodium, phosphorus, chlorine, potassium, and calcium with Ca/P ratio 1.47. The FTIR analysis identified hydroxyl, water molecules, carbonate, carbonyl, and phosphate groups in the sample. LC-MS analysis identified 49 active metabolites such as phenols, alkaloid, fatty acids and their derivatives, amino acids, carbohydrates, carboxylic acids, alcohols, and ketones from the sample. **Conclusion:** The characteristics of nanosuspension formulated with *Graptophyllum pictum* (L.) Griff extract and hydroxyapatite are similar to those of natural bones.

Keywords

characterization, *Graptophyllum pictum*, hydroxyapatite, nanosuspension

Karakterisasi nano suspensi ekstrak *Graptophyllum pictum* (L.) Griff dan hidroksiapatit sebagai material bone graft: penelitian eksperimental laboratoris

ABSTRAK

Pendahuluan: Hidroksiapatit merupakan komponen utama mineral anorganik pada jaringan keras manusia dan telah banyak digunakan sebagai keramik di bidang biomedis ortopedi dan kedokteran gigi. Penambahan bahan alami seperti *Graptophyllum pictum* dapat meningkatkan sifat antiinflamasi karena adanya senyawa fenolik dan alkaloid. Tujuan penelitian ini adalah mengetahui karakterisasi nanosuspensi yang diformulasikan dengan ekstrak *Graptophyllum pictum* (L.) Griff dan hidroksiapatit. **Metode:** Nanosuspensi dikarakterisasi menggunakan Scanning Electron Microscopy (SEM), Electron Dispersive X-ray analysis (EDX), Fourier Transform Independent Spectroscopy (FTIR), dan Liquid Chromatography Mass Spectrometry (LCMS). Evaluasi ini dilakukan untuk menunjukkan morfologi permukaan, komposisi unsur, gugus fungsi, dan mengidentifikasi metabolit aktif nanosuspensi. **Hasil:** SEM menunjukkan aglomerasi morfologi partikel hidroksiapatit berbentuk bulat. Analisis EDX menunjukkan kandungan karbon, oksigen, natrium, fosfor, klorin, kalium, dan kalsium dengan rasio Ca/P 1,47. Analisis FTIR mengidentifikasi gugus hidroksil, molekul air, karbonat, karbonil, dan fosfat dalam sampel. Analisis LC-MS mengidentifikasi 49 metabolit aktif seperti fenol, alkaloid, asam lemak dan turunannya, asam amino, karbohidrat, asam karboksilat, alkohol, dan keton dari sampel. **Simpulan:** Karakteristik nanosuspensi yang diformulasikan dengan ekstrak *Graptophyllum pictum* (L.) Griff dan hidroksiapatit mirip dengan tulang alami.

Kata kunci

karakterisasi, *Graptophyllum pictum*, hidroksiapatit, nanosuspensi

INTRODUCTION

Injuries to the oral cavity tend to arise from accidents, trauma, pathophysiological diseases, or dental procedures like tooth extraction. Extraction of a tooth will result in resorption of the alveolar bone, leading to alterations in the morphology of the alveolar bone.¹ According to the 2011 Household Health Survey conducted by the Indonesian Ministry of Health, the occurrence of bone and periodontal damage accounted for 60% of dental and oral cases in Indonesia. Untreated and increasing alveolar bone resorption can result in oral health complications such as tooth mobility and subsequent tooth loss.² Socket preservation is a procedure that involves placing graft material into the empty space left after a tooth is extracted.³ The objective of socket preservation is to minimize alterations in the proportions of the alveolar ridge and ensure adequate bone volume for the implantation of dental implants. Several studies have shown that socket preservation is effective in reducing ridge resorption compared to control sites that did not undergo alveolar bone socket preservation.^{4,5}

One method of therapy for alveolar bone injury is the utilization of bone graft. Utilizing bone grafts can effectively halt the progression of alveolar bone deterioration and expedite the process of alveolar bone regeneration, which involves the development of new cementum tissues, periodontal ligaments, and alveolar bone. Hydroxyapatite is frequently employed as a bone graft material in socket preservation. Hydroxyapatite is a very stable calcium phosphate molecule that maintains its structure and properties even under varying temperature, pH, and composition conditions in the bloodstream. It is derived from calcium phosphate and shares a chemical formula and features comparable to the inorganic minerals present in bones and teeth.^{6,7} Hydroxyapatite, a mineral similar to bones and teeth, is extensively researched in biomedical fields due to its biological advantages such as biocompatibility, bioaffinity, bioactivity, osteoconduction, osteointegration, and its lack of local or systemic toxicity.^{8,9}

In bone tissue engineering construction, bioactive properties were required to stimulate regenerative processes and tissue-specificity. The combination of scaffolds and bioactive compounds attracts and aggregates stem cells to bone damage areas, promoting osteogenic differentiation.^{10,11} In recent years, numerous studies have been conducted to integrate herbal plant extracts into tissue engineering constructs due to their bioactive properties, environmental sustainability, potential non-toxicity, affordability, and ease of extraction.¹² One such plant, *Graptophyllum pictum* (L.) Griff., shows promise as a potent antioxidant, antimicrobial, antifungal, and anti-inflammatory agent.¹³

Graptophyllum pictum (L.) Griff, referred to as purple leaves, belongs to the *Acanthaceae* family. It has been registered as a medicinal plant in the pharmacopoeia's second edition in 2017 and used in traditional medicine to treat various diseases.¹⁴ Phenolic and flavonoid phytochemical compounds found in *Graptophyllum pictum* (L.) Griff have anti-inflammatory properties that work by reducing free radicals and blocking enzymes involved in inflammatory processes, like cyclooxygenase-2 and inducible nitric oxide synthase. More studies reveal that *Graptophyllum pictum* (L.) Griff contains volatile compounds, tannins, alkaloids, terpenoids, and metabolites of the steroid class that are useful in the treatment of infections.¹⁵

This study created nanosuspension of *Graptophyllum pictum* (L.) Griff extract and hydroxyapatite. The main objective of using nanosuspension is to enhance the absorption and bioavailability properties. Therefore, the main purposes of the present study are to evaluate the physicochemical properties of the *Graptophyllum pictum* (L.) Griff extracts and hydroxyapatite combination to create a nanosuspension. To the best of our knowledge, no prior research has been done in the literature to examine this phenomenon and assess how the inclusion of *Graptophyllum pictum* (L.) Griff extracts affects the properties of the scaffolds that are created.

METHODS

This study was conducted over the period from March to May 2024. The production of purple leaf extract (*Graptophyllum pictum* (L.) Griff) was conducted at the Biology Department, Faculty of Mathematics and Natural Sciences, Katolik Widya Mandala University. The purple leaves were sourced from the UPT Herbal Materia Medica Laboratory in Batu, East Java Province. A total of 600 grams of leaves were subjected to an extraction process using 2 liters of 96% ethanol, with the mixture left to stand at room temperature in a closed container for three days. Afterward, the mixture was filtered using filter paper to obtain the macerate, and the remaining pulp was evaporated to produce a concentrated extract of purple leaves.¹⁶

The nanosuspension sample was prepared at the Pharmacy Academy of Surabaya by first adding 10 ml of hot distilled water to the mortar, followed by the addition of 1 gram of sodium carboxymethyl cellulose (CMC Na), which was left to stand for 15 minutes. The mixture was stirred until a gel mass was formed. Separately, 1 gram of nipagin solution was dissolved in 10 ml of distilled water and added to the gel mass. A previously prepared extract solution, consisting of 1 g of extract dissolved in 20 ml of 96% ethanol, was stirred until homogeneous in the mortar. Hydroxyapatite (nanoXIM®HAp200, FLUIDINOVA, Portugal) was added to the mortar and stirred until homogeneous. Next, 100 g of distilled water was added and stirred for 10 minutes. The nanosuspension was stirred at a speed of 1400 rpm for 90 minutes at 50°C.¹⁷

Characterization was performed at two different locations: SEM-EDX and FTIR analyses were conducted at the Material Characterization Division, Department of Materials and Metallurgical Engineering, Sepuluh Nopember Institute of Technology in Surabaya, while LC-MS analysis was carried out at the Metabolomics Laboratory, Superior Research Laboratory Unit, Bogor Agricultural University. Morphology and Ca/P ratio of the sample were detected by SEM-EDX. The sample is placed on a carbon-tipped pin holder so that the sample sticks to the holder, then the sample is inserted into the EDX tool. After the SEM and EDX software were connected to the computer, the data from the sample was collected. Functional groups present in nanosuspension sample were detected by FTIR program, namely OMNIC. The sample graphic results were obtained. The FTIR results are in the form of graphs that are read by matching the peak tab.¹⁸

The LC-MS test was carried out to identify chemical compounds in the nanosuspension. The nanosuspension was diluted 1:2 with methanol, then filtered with a 0.2 µm Nylon membrane. A total of 2 µL of sample filtrate was injected into the LC-MS instrument system. The eluent used was [H₂O + 0.1% formic acid (A) and acetonitrile + 0.1% formic acid (B)] with a total flow rate of 0.2 mL/minute. The gradient method used is 0-1 minute (5% B), 1-25 minutes (5-95% B), 25-28 minutes (95% B), 28-33 minutes (5% B). The stationary phase consists of Accucore C18, 100 x 2.1 mm, 1.5 µm (ThermoScientific) at a temperature of 30°C.

The instrument is set so that LC-MS/MS analysis data can then be processed using Compound Discoverer 3.2 software and matched with the MS1 and MS2 output spectra using various online databases (mzCloud, ChemSpider, and PubChem) to obtain predictions of the chemical structure of metabolites. Detecting masses measuring 100-1,500 m/z using the negative ionization method.¹⁹

RESULTS

Size distribution of the nanosuspension formulated with *Graptophyllum pictum* (L.) Griff extract and hydroxyapatite was measured by Particle Size Analyzer. The d.nm size of nanosuspension was determined as 21.6 d.nm (Figure 1).

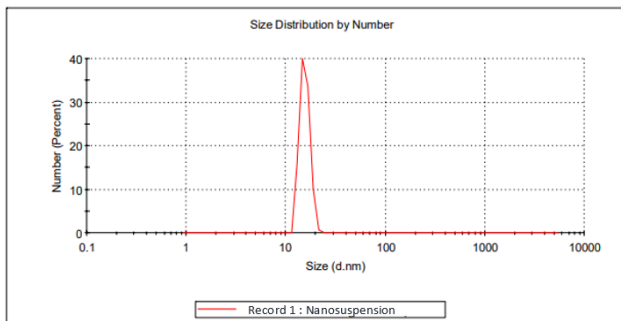


Figure 1. Particle Size Analyzer test results on the combination nanosuspension of purple leaf extract and hydroxyapatite

The combination nanosuspension sample of *Graptophyllum pictum* extract and hydroxyapatite was observed using SEM with magnification of 2,500x, 7,500x, 10,000x, and 20,000x. The SEM test results can be seen in Figure 2 which shows the morphology of the sample. The image shows the agglomeration of spherical hydroxyapatite particles towards granular.

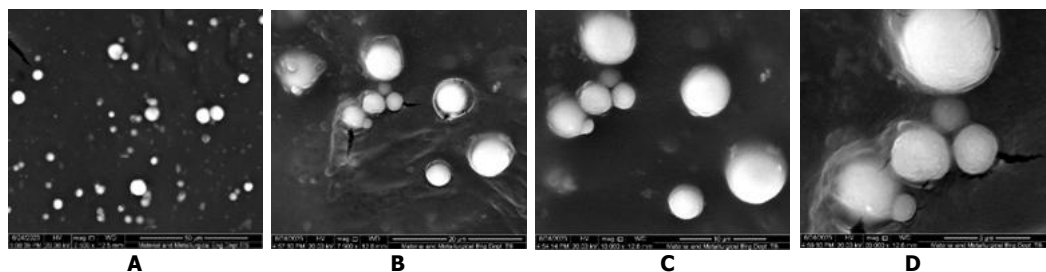
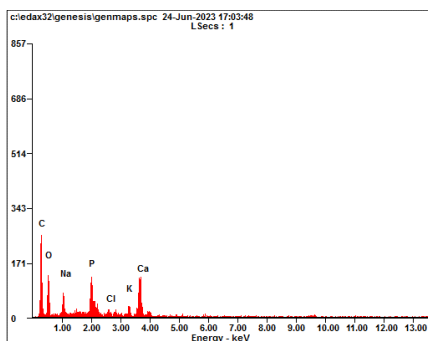


Figure 2. SEM results show the morphology of nanosuspension formulated with *Graptophyllum pictum* (L.) Griff extract and hydroxyapatite at magnification: A. 2.500 x; B. 7.500 x; C. 10.000 x; and D. 20.000x

The results of the EDX analysis can be seen in Figure 3 which shows that there is a content of Carbon (C; 33.13%), Oxygen (O; 33.73%), Sodium (Na; 7.08%), Phosphorus (P; 7.67%), Chlorine (Cl; 01.25%), Potassium (K; 2.58%), and Calcium (Ca; 14.56%). Based on the results of the EDX analysis, the comparison value of the calcium and phosphate molecule ratio (Ca/P ratio) was also obtained at 1.47. This value is lower than the stoichiometric ratio of hydroxyapatite Ca/P (1.67).



Element	Wt%	At%
CK	33.13	46.86
OK	33.73	35.82
NaK	07.08	05.23
PK	07.67	04.20
ClK	01.25	00.60
KK	02.58	01.12
CaK	14.56	06.17
Matrix	Correction	ZAF

Figure 3. The result of EDX shows the composition of nanosuspension

FTIR analysis was carried out to determine the functional groups contained in the test sample of the nanosuspension formulated with *Graptophyllum pictum* (L.) Griff extract and

hydroxyapatite. The IR transmission spectrum of the sample is shown in Figure 4. Table 1. shows the wave numbers of the functional groups possessed by the sample. Based on Table 1, there is a hydroxyl group (OH^-) which is marked by a peak at wave number 3320.61 cm^{-1} , water molecules (H_2O) at wave number 2167.30 and phosphate group (PO_4^{3-}) at wave number 1015.78 and 571.69. The results of FTIR analysis also show the presence of a carbonate group (CO_3^{2-}) at wave number 1381.53. In this spectrum, the carbonyl group ($\text{C}=\text{O}$) indicates the presence of one of the functional groups of the metabolite compounds found in purple leaves.

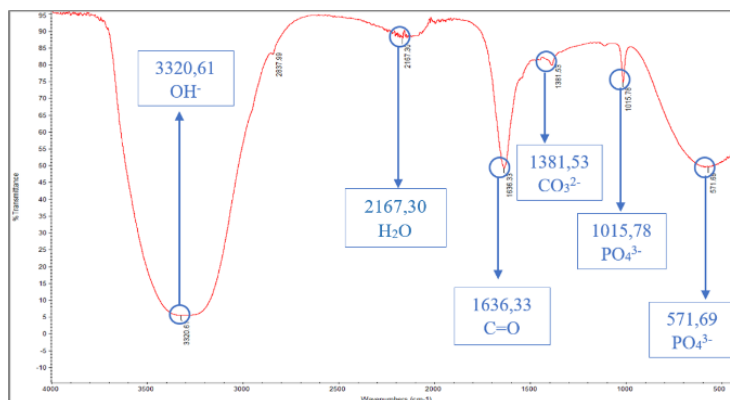


Figure 4. Result of FTIR spectrum of nanosuspension formulated with *Graptophyllum pictum* (L.) Griff extract and hydroxyapatite

Table 1. Characteristic bands of nanosuspension formulated with *Graptophyllum pictum* and hydroxyapatite identified from the FTIR spectrum.

Wavelength (cm ⁻¹)	Standard Range (cm ⁻¹)	Functional Group	Description	References
3320,61	3500-3000	OH^-	Stretching vibration	20
2167,30	2100-2182	H_2O	Water molecule	21,22
1636,33	1760-1600	$\text{C}=\text{O}$ (amide I)	Stretching	23
1381,53	1366-1388	CO_3^{2-}	Substitutes phosphatase ion	22,24
1015,78	1200-1000, 1100-1000	PO_4^{3-}	Stretching mode	20,25
571,69	520-660	PO_4^{3-}	Bending mode	26

Analysis of metabolites from samples was carried out using LC-MS/MS based on differences in the polarity of the ethanol solvent. The presence of peaks that appeared in the chromatogram showed the presence of 49 different compounds from nanosuspension formulated with *Graptophyllum pictum* (L.) Griff extract and hydroxyapatite (Figure 5). The metabolic compounds that were successfully identified were based on parameters such as molecular weight, chemical formula of the compound, and retention time. A total of 49 active metabolites were found in the samples. The profiling process was carried out to separate secondary metabolites from impurities as well as to determine the chemical structure of metabolites using the PubChem, ChemSpider and mzCloud databases.

After the profiling process 49 compounds are divided into several groups (Table 2), namely phenols (5), alkaloids (3), fatty acids and their derivatives (15), amino acids (9), carbohydrates (4), carboxylic acids (8), alcohols (1), ketones (2), and other compounds (14).

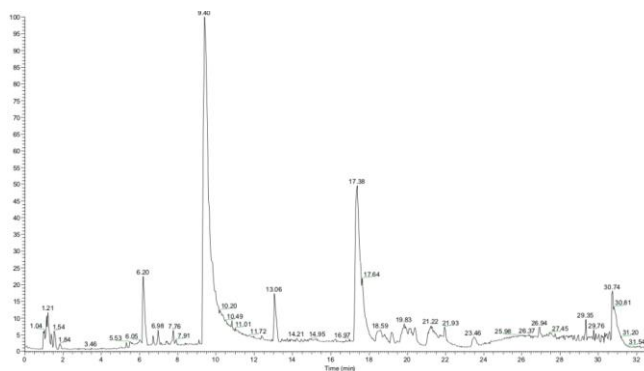


Figure 5. LC-MS chromatogram of nanosuspension formulated with *Graptophyllum pictum* and hydroxyapatite

Table 2. Metabolite compound content from LC-MS analysis

Class	Compound	RT (min)	Formula	Molecule Weight (g/mol)
Amino acid	Ac-N(Me)Phe-Ala-Leu-Gly-OH	9.197	C23 H34 N4 O6	462,2469
Phenol	Acetophenone, (2,4-dinitrophenyl)hydrazone	5.606	C14 H12 N4 O4	300,0846
Other	Aderbasib	9.174	C21 H28 N4 O5	416,2049
Amino acid	Ala-Ser-Tyr-Thr	7.977	C19 H28 N4 O8	440,1895
Carbohydrate	Arabic acid	1.247	C5 H10 O6	166,047
Carboxylic acid	Benzoic acid	9.513	C7 H6 O2	122,0358
Amino acid	Bicine	1.253	C6 H13 N O4	163,0837
Other	Butopyronoxyl	7.763	C12 H18 O4	226,1202
Carboxylic acid	Carboxycytosine	9.443	C5 H5 N3 O3	155,0336
Phenol	Catechol	9.445	C6 H6 O2	110,0358
Amino acid	Cbz-Lys-D-gGlu-Oic-OH	10.132	C28 H40 N4 O8	560,2833
Fatty acid	Citraconic acid	1.922	C5 H6 O4	130,0257
Fatty acid	Corchorifatty acid F	12.49	C18 H32 O5	328,2251
Other	Denipride	7.991	C18 H26 N4 O5	378,1891
Carbohydrate	D-(+)-Maltose	1.244	C12 H22 O11	388,1219
Carbohydrate	D-(+)-Galactose	1.245	C6 H12 O6	180,0628
Carboxylic acid	DL-Malic acid	1.27	C4 H6 O5	134,0206
Amino acid	Falgpa	9.383	C23 H32 N4 O7	476,2258
Phenol	Gentisic acid	9.448	C7 H6 O4	154,0258
Amino acid	Glu-Trp-Glu	7.846	C21 H26 N4 O8	462,1741
Carboxylic acid	kresoxim-methyl	10.444	C18 H19 N O4	313,1315
Other	Lignogliride fumarate	8.471	C20 H26 N4 O5	402,1891
Carboxylic acid	Methylmalonic acid	1.635	C4 H6 O4	118,0256
Other	N-carbobenzyloxy-prolyl-leucyl-glycine (N-hydroxy)amide	7.56	C21 H30 N4 O6	434,2154
Alcohol	NP-016596	7.058	C19 H30 O8	432,1996
Other	O-[3-(3-methoxypropyl)-5,6-dimethyl-2-thioxo-2,3-dihydro-4-pyrimidinyl] N,N-diethylcarbamothioate	11.157	C15 H25 N3 O2 S2	343,142
Phenol	Salicylic acid	9.912	C7 H6 O3	138,0308
Carboxylic acid	Terephthalic acid	6.29	C8 H6 O4	166,0259
Fatty acid	Traumatic Acid	13.125	C12 H20 O4	228,1359
Fatty acid	(15Z)-9,12,13-Trihydroxy-15-octadecenoic acid	13.163	C18 H34 O5	330,2407
Fatty acid	(+/-)-9,10-dihydroxy-12Z-octadecenoic acid	19.984	C18 H34 O4	296,2351
Fatty acid	(±)9-HpODE	17.465	C18 H32 O4	312,2301
Keton	{(1R,2R)-2-[(2Z)-5-(Hexopyranosyloxy)-2-penten-1-yl]-3-oxocyclopentyl}acetic acid	7.486	C18 H28 O9	388,1736
Other	1,2-Benzenedicarbonyldiazide	1.242	C8 H4 N6 O2	216,0398
Amino acid	2-(acetilamino)-3-(1H-indol-3-yl)propanoic acid	8.813	C13 H14 N2 O3	246,1004
Alkaloid	2-nitrosopyrimidine	9.445	C4 H3 N3 O	109,028
Other	2-[4-(methoxycarbonyl)piperazin-1-yl]-5-(0-methyl-.beta.,D-glucopyranosyloxy)pyrimidine	5.398	C17 H26 N4 O8	414,1738
Other	Propargyl-PEG8-acid	7.089	C20 H36 O10	436,2309
Alkaloid	4-Indolecarbaldehyde	9.428	C9 H7 N O	145,0519
Amino acid	4-Oxoproline	1.485	C5 H7 N O3	129,0417

Other	4-(3,5-dinitrothiophen-2-yl)pyrimidine	9.487	C8 H4 N4 O4 S	251,9945
Alkaloid	4,4',4''-[nitriлотris(methylene)]tris-1H-1,2,3-triazole-1-acetic acid triethyl ester	9.465	C21 H30 N10 O6	518,2363
Keton	4,5-Dihydroxy-3-oxo-1-cyclohexene-1-carboxylic acid	9.448	C7 H8 O5	172,0364
Fatty acid	12-HSA	22.047	C18 H36 O3	300,2664
Fatty acid	13(S)-HOTrE	18.72	C18 H30 O3	294,2194
Fatty acid	13(S)-HpOTrE	19.272	C18 H30 O4	292,2039
Fatty acid	15,16-DiHODE	20.469	C18 H32 O4	312,2301
Fatty acid	16-Hydroxyhexadecanoic acid	24.129	C16 H32 O3	272,2352
Other	O-[3-(3-methoxypropyl)-5,6-dimethyl-2-thioxo-2,3-dihydro-4-pyrimidinyl] N,N-diethylcarbamoithoate	10.64	C15 H25 N3 O2 S2	343,1388

DISCUSSION

The SEM test results show that the morphology of nanosuspension formulated with *Graptophyllum pictum* (L.) Griff extract and hydroxyapatite is round and has some agglomeration. The formation of this agglomeration is thought to be related to the presence of *Graptophyllum pictum* extract. This is in accordance with research by Nagaraj et al (2022) which states that the form of agglomeration indicates the presence of polydispersity in hydroxyapatite because the chemicals contained in *Tridax procumbens* leaf extract cover the hydroxyapatite.³⁰ The surface area and bioactivity of synthetic materials are greatly influenced by their size and shape.²⁷

There is always a need to reduce the size of hydroxyapatite crystals to the nanoscale in various hydroxyapatite applications. This is because materials with a smaller size (crystal size) are more reactive and have increased physicochemical properties because the exposed surface area is greater. This positions synthesized materials of nanoscale size favorably as a better choice.²⁸ Based on particle size testing, the average particle size of the sample is 21.6 nm which is included in the nanoparticle group. Nanoparticles are materials that have a particle size with ranging between 1-500 nm.²⁹

EDX analysis with elemental maps used to emit the elemental composition of the combination nanosuspension sample of *Graptophyllum pictum* extract and hydroxyapatite. The presence of oxygen atoms (O), calcium (Ca), and phosphorus (P) indicates the elemental composition of hydroxyapatite.²⁶ In addition, sodium (Na) was detected in the analysis, serving as one of the trace elements in the inorganic phase that contributes to bone strength and rigidity. The presence of Na is attributed to the use of CMC Na, which acts as a thickening, emulsifying, and stabilizing agent in the nanosuspension.

The presence of potassium (K), chlorine (Cl), and carbon (C) probably comes from *Graptophyllum pictum* extract. These three elements were also found in *Azadirachta indica* stem extract and *Tridax procumbens* leaves.^{30,31} In the results of the analysis of the nanosuspension formulated with *Graptophyllum pictum* (L.) Griff extract and hydroxyapatite, a combination of both molecular elements from hydroxyapatite and purple leaves was found. Therefore, from the EDX test results it can be concluded that the nanosuspension successfully contains *Graptophyllum pictum* extract and hydroxyapatite elements.

In addition to the content of elements in the nanosuspension, the EDX test results also display the atomic percentage (At%) of each element in the nanosuspension. The EDX results can be used to determine the Ca/P ratio. The comparison of Ca/P ratio values in the nanosuspension containing *Graptophyllum pictum* (L.) Griff extract and hydroxyapatite revealed a value of 1.47, which means $1.67 - 1.47 = 0.2$ Ca/P was lost or replaced. Non-stoichiometric hydroxyapatite may have an imbalance in calcium or phosphorus content. Additionally, hydroxyapatite that contains trace elements such as sodium (Na), magnesium (Mg), strontium (Sr), iron (Fe), aluminum (Al), and zinc (Zn) typically has a reduced Ca/P ratio.³² This is further evidenced by the detection of Na, Cl, and K elements in the EDX results,

indicating the presence of impurities. The presence of those element replaces a small portion of the Ca element in $\text{Ca}_{10}(\text{PO}_4)_6(\text{OH})_2$, causing the Ca/P ratio to be less than 1.67.³³

Based on the FTIR test, the presence of hydroxyl (OH^-), carbonate (CO_3^{2-}), phosphate (PO_4^{3-}), and water (H_2O) functional groups could be identified. The hydroxyl group (OH^-) comes from the presence of hydrated inorganic compounds. The PO_4^{3-} , OH^- , and CO_3^{2-} functional groups are the main components in the formation of hydroxyapatite.³⁴ This is consistent with the findings of Alves et al.³⁵ which demonstrated that commercial hydroxyapatite (nanoXIM®HAp.202) exhibited both intramolecular and intermolecular O-H stretching vibrations.

Furthermore, the hydroxyapatite displayed bending and stretching vibrations associated with the phosphate group (PO_4^{3-}).³⁵ Water molecules were detected at wave number 2167.30 cm^{-1} . This is possible because the surface sample absorbs water. The P-OH groups found on the surface of hydroxyapatite contribute to the adsorption of various molecules such as H_2O .³⁶ Meanwhile, the carbonate group detected probably came from CO_2 in the air, which reacts with calcium to form bonds so that a calcium carbonate phase appears during synthesis.³⁷

Apart from this functional group, another functional group appears, namely the carbonyl group ($\text{C}=\text{O}$) which was detected at a wave number of 1636.33 cm^{-1} . This functional group was detected in the wave number range of $1600\text{--}1760 \text{ cm}^{-1}$, indicating the presence of aldehyde, ketone and ester compounds originating from the extract.²³ The results of this research are in line with studies published by Muhaimin et al.,³⁷ which states that the $\text{C}=\text{O}$ group was detected at a wave number of 1639.49 cm^{-1} , which indicates the presence of one of the functional groups of the metabolite compounds contained in betel leaves.³⁷

Graptophyllum pictum extract mainly contains phenols, flavonoid, alkaloids, fatty acids, amino acids.¹⁵ Several studies have investigated the therapeutic values of *Graptophyllum pictum* leaf, which have been shown to possess in vitro anti-inflammatory and antioxidant.³⁸ In this study, the chemical constituents of *Graptophyllum pictum* extract in combination of nanosuspension between purple leaf extract and hydroxyapatite were analyzed using LCMS. Prediction compounds are thought to be groups of phenols compounds, alkaloids, fatty acids, amino acids compounds. This is similar to the phytochemical screening of *Graptophyllum pictum* that contain classes of these compound.¹⁵ This indicates that the nanosuspension that has been made contains the bioactive compound of purple leaves.

CONCLUSION

The nanosuspension formulated with *Graptophyllum pictum* (L.) Griff extract and hydroxyapatite shows promising potential as a novel bone graft material especially for socket preservation. The nanosuspension showed round morphology, agglomerated hydroxyapatite, a non-stoichiometric Ca/P ratio 1.47 suggest structural compatibility with natural bone. In addition, there is potential bonding between components, indicating good material integration. Additionally, the presence of bioactive compounds with anti-inflammatory and antioxidant properties, likely from the plant extract, may create a favorable environment for bone healing.

Author Contribution: Conceptualization, K.B.; methodology, K.B. and R.M.; software, K.B and R.M.; validation, D.R.; formal analysis, K.B. and R.M.; investigation, K.B.; resources, R.M.; data curation, K.B. and R.M.; writing—original draft preparation, K.B.; writing—review and editing, R.M.; visualization, K.B.; supervision, D.R.; project administration, K.B.; funding acquisition, D.R. All authors have read and agreed to the published version of the manuscript.

Funding: The research was funded by the Ministry of Research, Technology and Higher Education of the Republic of Indonesia (Kemenristekdikti RI) (letter of appointment agreement number: 1620/B/UN3.LPPM/PT.01.03/2024)

Ethical Approval: This study has been approved by the ethical health committee of the Faculty of Dental Medicine, Universitas Airlangga with number of certificate No: 0673/HRECC.FODM/VII/2024.

Institutional Review Board Statement: Not applicable

Informed Consent Statement: Not applicable

Data Availability Statement: The availability of research data will be provided with the permission of all researchers via email correspondence with due regard to ethics in research.

Conflicts of Interest: The authors declare no conflict of interest.

REFERENCES

- Lee H, Noh K, Lee DW. Bone regeneration in the extraction socket filled with atelocollagen: histological and radiographic study in beagle dogs. *J Korean Dent Sci.* 2016;9(2):55–62. <https://doi.org/10.5856/jkds.2016.9.2.55>
- Nurlindah Hamrun, Alya Hilda Saifuddin, Alya Khaerunnisa I Day, Hemayu Aditung, Sri Handayani Saharuddin, Megatriani Matandung, et al. Role of fucoidan in stimulating osteoblast cells in alveolar bone loss. *Makassar Dent J.* 2022;11(2):229–34. <https://doi.org/10.35856/mdj.v11i2.602>
- Annunziata M, Guida L, Natri L, Piccirillo A, Sommesse L, Napoli C. The Role of Autologous Platelet Concentrates in Alveolar Socket Preservation: A Systematic Review. *Transfusion Medicine and Hemotherapy.* 2018;45(3):195–203. <https://doi.org/10.1159/000488061>
- Udeabor SE, Heslich A, Al-Maawi S, Alqahtani AF, Sader R, Ghanaati S. Current Knowledge on the Healing of the Extraction Socket: A Narrative Review. *Bioengineering (Basel).* 2023;10(10):1145. <https://doi.org/10.3390/bioengineering10101145>
- Yip I, Ma L, Mattheos N, Dard M, Lang NP. Defect healing with various bone substitutes. *Clin Oral Implants Res.* 2015;26(5):606–14. <https://doi.org/10.1159/000488061>
- Halim NAA, Hussein MZ, Kandar MK. Nanomaterials-upconverted hydroxyapatite for bone tissue engineering and a platform for drug delivery. *Int J Nanomedicine.* 2021;16:6477–96. <https://doi.org/10.2147/IJN.S298936>
- Sano T, Kuraji R, Miyashita Y, Yano K, Kawanabe D, Numabe Y. Biomaterials for Alveolar Ridge Preservation as a Preoperative Procedure for Implant Treatment: History and Current Evidence. *Bioengineering.* 2023;10(12):1376. <https://doi.org/10.3390/bioengineering10121376>
- Kattimani VS, Kondaka S, Lingamaneni KP. Hydroxyapatite—Past, Present, and Future in Bone Regeneration. *Bone Tissue Regen Insights.* 2016;7:BTRI.S36138. <https://doi.org/10.4137/btri.s36138>
- Shi H, Zhou Z, Li W, Fan Y, Li Z, Wei J. Hydroxyapatite Based Materials for Bone Tissue Engineering: A Brief and Comprehensive Introduction. *Crystals.* 2021;11(2):149. <https://doi.org/10.3390/cryst11020149>
- Safari B, Davaran S, Aghanejad A. Osteogenic potential of the growth factors and bioactive molecules in bone regeneration. *Int J Biol Macromol.* 2021;175:544–557. <https://doi.org/10.1016/j.ijbiomac.2021.02.052>
- Bretschneider H, Quade M, Lode A, Gelinsky M, Rammelt S, Vater C. Chemotactic and angiogenic potential of mineralized collagen scaffolds functionalized with naturally occurring bioactive factor mixtures to stimulate bone regeneration. *Int J Mol Sci.* 2021;22(11). <https://doi.org/10.3390/ijms22115836>
- Fatehi P, Abbasi M. Medicinal plants used in wound dressings made of electrospun nanofibers. *J Tissue Engineering and Regenerative Medicine.* 2020;4:1527–48. <https://doi.org/10.1002/term.3119>
- Rachim SA, Kurniawati A, Astuti P. The Effect of Purple Leaf Extract (*Graptophyllum pictum* L. Griff) to The Amount of Fibroblast in Gingiva Rat Wistar induced by *Porphyromonas gingivalis*. *Dent J Ked Gi.* 2020;14(2):94–100. <https://doi.org/10.30649/denta.v14i2>
- Goswami M, Ojha A, Mehra M. A Narrative literature review on Phytopharmacology of a Caricature Plant: *Graptophyllum pictum* (L.) Griff. (Syn: *Justicia picta* Linn.). *Asian Pac. J. Health Sci.* 2021;8(3):44–7. <https://doi.org/10.21276/apjhs.2021.8.3.10>
- Makkiyah FA, Rahmi EP, Mahendra FR, Maulana F, Arista RA, Nurcholis W. Polyphenol content and antioxidant capacities of *Graptophyllum pictum* (L.) extracts using in vitro methods combined with the untargeted metabolomic study. *J Appl Pharm Sci.* 2024;14(3):55–63. <https://doi.org/10.7324/JAPS.2024.153548>
- Brahmantyo MR, Nirwana I, Rianti DD. Application of purple leaf extract (*Graptophyllum pictum*) in wound healing process of collagen density. *International Journal of Pharmaceutical Research.* 2020;12(4):1541–5. <https://doi.org/10.31838/ijpr/2020.12.04.218>
- Nugraha AP, Triwardhani A, Sitalaksmi RM, Ramadhani NF, Luthfi M, Ulfa NM, et al. Phytochemical, antioxidant, and antibacterial activity of *Moringa oleifera* nanosuspension against peri-implantitis bacteria: An in vitro study. *J Oral Biol Craniofac Res.* 2023;13(6):720–6. <https://doi.org/10.1016/j.jobcr.2023.09.004>
- Rianti D, Kristanto W, Damayanti H, Putri TS, Dinaryanti A, Syahrom A, et al. The Characteristics and Potency of Limestone-based carbonate hydroxyapatite to Viability and Proliferation of Human Umbilical Cord Mesenchymal Stem Cell. *Res J Pharm Technol.* 2022;15(5):2285–92. <https://doi.org/10.52711/0974-360X.2022.00380>
- Abdullah A, Nurjanah N, Reyhan M. Identification and Profiling of Active Compounds from Golden Apple Snail's Egg Pigments. *J Pengolah Has Perikan Indones.* 2017;20(2):286. <https://doi.org/10.17844/jphpi.v20i2.17909>
- Sobczak-Kupiec A, Malina D, Piątkowski M, Krupa-Zuczek K, Wzorek Z, Tyliszczak B. Physicochemical and biological properties of hydrogel/gelatin/ hydroxyapatite PAA/G/HAP/AgNPs composites modified with silver nanoparticles. *J Nanosci Nanotechnol.* 2012;12(12):9302–11. <https://doi.org/10.1166/jnn.2012.6756>
- Fadli A, Akbar F, Putri P, Pratiwi DI, Muhara I. Hydroxyapatite Powder Prepared by Low Temperature Hydrothermal Method from Sea Shells. The 1st Conference on Ocean, Mechanical and Aerospace; 2014 Nov 19.
- Jackson P, Robinson K, Puxty G, Attalla M. In situ Fourier Transform-Infrared (FT-IR) analysis of carbon dioxide absorption and desorption in amine solutions. In: *Energy Procedia.* 2009. p. 985–94. <https://doi.org/10.1016/j.egypro.2009.01.131>
- Ganta DD, Hirpaye BY, Raghavanpillai SK, Member SY. Green Synthesis of Hydroxyapatite Nanoparticles Using Monoon longifolium Leaf Extract for Removal of Fluoride from Aqueous Solution. *J Chem.* 2022; 2022. <https://doi.org/10.1155/2022/4917604>
- Muhammad M, Marwan M, Munawar E, Zaki M. Experimental study of CO2 utilization as a density modification agent for maximizing palm shells and kernels separation efficiency. *S Afr J Chem Eng.* 2022;42:283–9. <https://doi.org/10.1016/j.sajce.2022.09.006>
- Kartikasari N, Yuliati A, Listiana I, Setijanto D, Suardita K, Ariani MD, et al. Characteristic of bovine hydroxyapatite-gelatin-chitosan scaffolds as biomaterial candidate for bone tissue engineering. 2016 IEEE EMBS Conference on Biomedical Engineering and Sciences. 2016. P. 623–

- 6.
26. Timchenko PE, Timchenko E V., Pisareva E V., Vlasov MY, Red'Kin NA, Frolov OO. Spectral analysis of allogeneic hydroxyapatite powders. In: J. Phys. Conf. Ser. Institute of Physics Publishing; 2017. <https://doi.org/10.1088/1742-6596/784/1/012060>
27. Prabhu S, Poulouse EK. Silver nanoparticles: mechanism of antimicrobial action, synthesis, medical applications, and toxicity effects. *Int Nano Lett.* 2012;2(1). <https://doi.org/10.1186/2228-5326-2-32>
28. Irwansyah FS, Noviyanti AR, Eddy DR, Risdiana R. Green Template-Mediated Synthesis of Biowaste Nano-Hydroxyapatite: A Systematic Literature Review. Vol. 27, *Molecules.* MDPI; 2022. <https://doi.org/10.3390/molecules27175586>
29. Yusuf A, Almotairy ARZ, Henidi H, Alshehri OY, Aldughaim MS. Nanoparticles as Drug Delivery Systems: A Review of the Implication of Nanoparticles' Physicochemical Properties on Responses in Biological Systems. *Polymers (Basel).* 2023;15(7). <https://doi.org/10.3390/polym15071596>
30. Nagaraj A, Kumar Kalagatur N, Kadirvelu K, Shankar S, Mangamuri UK, Sudhakar P, et al. Biomimetic of hydroxyapatite with *Tridax procumbens* leaf extract and investigation of antibiofilm potential in *Staphylococcus aureus* and *Escherichia coli*. *Indian J Biochem Biophys.* 2022;59:755–66.
31. Nagaraj A, Samiappan S. Presentation of Antibacterial and Therapeutic Anti-inflammatory Potentials to Hydroxyapatite via Biomimetic With *Azadirachta indica*: An in vitro Anti-inflammatory Assessment in Contradiction of LPS-Induced Stress in RAW 264.7 Cells. *Front Microbiol.* 2019;10. <https://doi.org/10.3389/fmicb.2019.01757>
32. Wu SC, Hsu HC, Wang HF, Liou SP, Ho WF. Synthesis and Characterization of Nano-Hydroxyapatite Obtained from Eggshell via the Hydrothermal Process and the Precipitation Method. *Molecules.* 2023;28(13). <https://doi.org/10.3390/molecules28134926>
33. Rahman RF, Maryana OFT, Effendi D. Optimasi Granul Hydroxyapatite Terdoping SrCO₃ Sebagai Anti-Bakteri Pada Aplikasi Bone Filler Dengan Menggunakan Metode Basah (Wet Method). 2020.
34. Hanura AB, Trilaksana W, Suptijah P. CHARACTERIZATION OF NANOHYDROXYAPATITE FROM TUNA'S *Thunnus sp* BONE AS BIOMATERIALS SUBSTANCE. *Jurnal Ilmu dan Teknologi Kelautan Tropis.* 2018; 9(2):619–29. <https://doi.org/10.29244/jitkt.v9i2.19296>
35. Alves BC, de Miranda RS, Frigieri BM, Zuccari DAPC, de Moura MR, Aouada FA, et al. A 3D Printing Scaffold Using Alginate/Hydroxyapatite for Application in Bone Regeneration. *Materials Research.* 2023; 26. <https://doi.org/10.1590/1980-5373-MR-2023-0051>
36. Alif MF, Arief S, Yusuf Y, Yunita Y, Ramadhani J, Triandini S. Synthesis of hydroxyapatite from *Faunus ater* shell biowaste. *Next Materials.* 2024; 3:100157. <https://doi.org/10.1016/j.nxmte.2024.100157>
37. Muhaimin FI, Cahyaningrum SE, Lawarti RA, Maharani DK. Characterization and Antibacterial Activity Assessment of Hydroxyapatite-Betel Leaf Extract Formulation against *Streptococcus mutans* In Vitro and In Vivo. *Indones. J. Chem.* 2023; 23(2):358–69. <https://doi.org/10.22146/jic.77853>
38. Jiangseubchatveera N, Liawruangrath B, Liawruangrath S, Teerawutgulrag A, Santiarworn D. The chemical constituents and the cytotoxicity, antioxidant and The chemical constituents and the cytotoxicity, antioxidant and antibacterial activities of the essential oil of *Graptophyllum pictum* (L.) Griff antibacterial activities of the essential oil of *Graptophyllum pictum* (L.) Griff. *J. Essent. Oil-Bear. Plants.* 2015; 18(1):11–7. <https://doi.org/10.1016/j.ces.2012.01.058>